





# Control Methods for Operation of Pumped Storage Plants with Full-size Back-to-Back Converter Fed Synchronous Machines

Raghendra Tiwari , *Student Member, IEEE*, Roy Nilsen , *Member, IEEE*, Olve Mo , and Arne Nysveen , *Senior Member, IEEE*

**Abstract**—A full-size converter-fed synchronous machine (CFSM) technology is emerging as the most flexible system for pumped storage plants for efficient operation in a wide range of water flows, which is not the case in existing power plants with fixed-speed synchronous machines. This article presents steady-state control strategies to execute the variable speed operation of the pumped storage power plants in both turbine and pump mode using a full-size back-to-back converter. Furthermore, the starting method of the power plant in pump and turbine mode from a standstill is proposed. In addition, the seamless transition of operating modes from the turbine to pump mode and vice versa is presented, which is an essential feature required to adapt to the varying power generation from renewable energy sources like solar and wind. The behavior of the power plant during a voltage dip on ac grid, and the low-voltage ride-through (LVRT) capability in both turbine and pump modes are also presented. The proposed control strategies are experimentally verified with a 100 kVA machine and converter setup with an emulated reversible pump turbine (RPT) and waterways.

**Index Terms**—Pumped storage power plant, Variable speed drives, Converter-fed Synchronous Machine, Reversible pump turbine.

## I. INTRODUCTION

In the past decade, the integration of renewable energy sources such as wind and solar into the grid has followed an unprecedented increasing trend and is continuing to do so [1]. To better utilize these pollution-free energy sources, pumped storage hydropower plants (PSHPs) with fixed-speed synchronous machine units are being considered for conversion to variable-speed operation. Even though the variable-speed operation of PSHPs exists with doubly fed induction machine (DFIM) technology, it takes several minutes (5–10 minutes) to start up the system in pump mode as the water inside the turbine casing needs to be blown down below the runner level. Additionally, changing the mode of operation from the turbine to the pump, and vice versa, requires altering the phase sequence of the stator winding. Hence, it takes even longer to switch from generation mode to pump mode and cannot exhibit a seamless transition [2]. Therefore, the demand to make the system dynamic to fully utilize renewable energy is going to be the ultimate objective. Since DFIM technology, which requires a converter of about 30% of the stator power rating, is not enough to serve this purpose, the full-size converter is the way forward while converting the fixed-speed pumped storage plants to variable speed operation [3], [4].

The semiconductor device technology is rapidly increasing and manufacturers are continuously improving the rated capacity of high-voltage - high-current devices. This has led to the attainment of high-power converters with multi-level converter topologies. Hence, a full-size converter to the stator of existing synchronous machines (SMs) in the fixed-speed PSHPs can make the plant dynamic and more efficient. The first of this type is installed in one of the 100 MW units of Grimsel-2 PSHP, Switzerland to run in pump mode [5]. Recently, a full-size direct ac / ac modular multilevel converter (MMC) of 80 MW is installed at the Malta Upper Stage Project in Austria to enable the variable speed operation of the existing fixed-speed generation unit [6].

Although full-size converter technology for PSHPs is the most favored topic in the energy storage market, control-associated challenges have not been thoroughly discussed in the literature. The control strategy for a PSHP with DFIM technology is investigated using simulation tools in [7]. The higher-level control strategy in pump mode for an MMC-based full-size converter is discussed with simulation results in [8].

The control aspects of the full-size converter-fed synchronous machine (CFSM) to enable fast startup, and fast transition of operational mode from the turbine to pump and vice versa are presented in [9]. In this article, these earlier results are extended to address further operational challenges like low-voltage ride-through (LVRT) in both the turbine and pump mode of operation and are validated through experimental results, which are the main contributions of this article. A set of outer layer (secondary) control strategies for both grid and machine side converters for generating (turbine) mode, pumping mode, and fast transition from the turbine to pump mode and vice versa have been proposed for the dynamic control of power in both modes. The control strategies are validated using experimental results from a laboratory prototype consisting of a 100 kVA converter-fed synchronous machine and an induction machine of similar size to emulate a reversible pump turbine (RPT). Since the secondary controller is independent of the type of converter topology, a two-level three-phase converter is used on each side of the back-to-back converter setup in the laboratory.

This article is subsequently organized as follows—Section II reviews the converter topologies which meet the requirements of the full-size CFSM technology. In section III, the control strategy for the secondary controller, efficiency optimization algorithm, and for grid-side and machine-side converters are

described. Section IV presents the modeling equations of an RPT which is implemented in an induction machine set to emulate the behavior in the laboratory setup. Section V presents the experimental results from a 100 kVA back-to-back CFSM setup on seamless mode transition and LVRT capability. The conclusions of this paper are presented in Section VI.

## II. CONVERTER TOPOLOGIES

With the development of high voltage high current devices like IGBTs, high-power converters of up to 100 MVA are commercially viable [10]. In Grimsel-2, two 50 MVA three-level Active Neutral Point Clamped (ANPC) converters are installed to enable variable speed operation of one of the four 100 MVA units [3]. For a 100 MVA unit of PSHP, the stator voltage rating of synchronous machines is in the range of 13–15 kV. Converter topologies with three-level Neutral Point Clamped (NPC) and ANPC are the most popular medium voltage industrial drives, and hence, can also be used in this application for both grid-side and machine-side. Since the grid-side converter is connected to a fixed frequency AC grid, a three-level NPC converter or an MMC can be preferred [11]. But on the machine side, the output frequency varies as the speed varies from +100% in turbine mode to -100% in pump mode (speed in pump mode may reach -120% depending upon the net head). The load torque also varies with the speed of rotation of the RPT as presented in Fig.1. The torque required with a minimum opening of guide vanes is typically around 13%, which is considered as the torque requirement for the converters to start the RPT in pump mode from a standstill. This torque is sufficient to accelerate the RPT with water in the turbine casing which is not the case in any existing pumped storage plants.

As discussed in [12], around a 100 MVA of three-level ANPC converter can be achieved in a single converter block. And such a converter can provide a starting torque of around 60% of the rated torque. In the past decade, numerous research has been carried out to apply MMC in drive applications and has shown promising results that it can provide a starting torque up to 40% of the rated torque [13]. Hence, MMC can also be considered an alternative for grid-side and machine-side converters.

## III. CONTROL STRATEGY

The full-size back-to-back CFSM comprises a hierarchical control structure where the lowermost control layer (primary control) is the inner current controller which employs either pulse width modulation or hysteresis control loop, or direct torque control (DTC). The outer control loop (secondary control) is the layer that interacts with other systems, e.g. Transmission System Operator (TSO) in this case and it generates the references for the primary layer with the logic based on the mode of operation. The uppermost control layer (tertiary control) includes the global frequency or voltage regulation of a system normally controlled by a TSO in a large integrated grid network or by an automated system in a relatively smaller system.

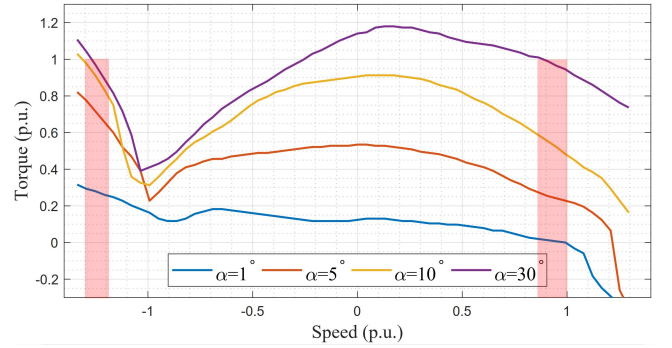


Fig. 1. Torque - Speed characteristics of a reversible pump turbine at varying guide vanes opening ( $\alpha$ ). The speed is positive in turbine (generating) mode and negative in pump (motoring) mode. The shaded regions show the rated operating area in respective modes. Courtesy: Water Power Laboratory, NTNU, Trondheim.

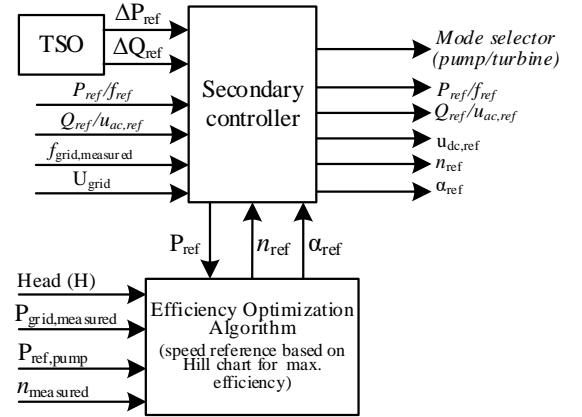


Fig. 2. Schematic showing secondary layer control strategies for the full-size back-to-back converters. The plant operator normally sets the active and reactive power references (input to the Secondary controller). These references are used as references for the primary (inner) controllers. The TSO provides an incremental change dynamically according to the instantaneous grid parameters. The Efficiency Optimization Algorithm processes the net head ( $H$ ), Power reference ( $P_{ref}$ ) in both turbine and pump mode and determines the optimal speed of rotation of the RPT. The references produced by the secondary controller are passed to the converter controllers presented in Fig. 3. A set of converter controllers is activated depending on the mode of operation (pump/turbine).

### A. Secondary Controller

The secondary controller serves as the local controller of the plant and provides frequency and voltage references for the grid-side converter; speed, and dc-link voltage references for the machine-side converter; and speed and guide vanes set-point to the turbine governor. The startup in the turbine or the pump mode and the transition between these modes is initiated by this controller. The overview of the interaction of the secondary controller with the other systems is shown in Fig. 2. The active and reactive power references ( $P_{ref}$  and  $Q_{ref}$ ) are set by the plant operator and the secondary controller passes it to the primary (inner) controller presented in Fig. 3.

### B. Efficiency Optimization Algorithm

The hydraulic turbines run at their maximum efficiency if the rotational speed is varied according to the variation in the water flow and the net head. Normally, the efficiency curves for

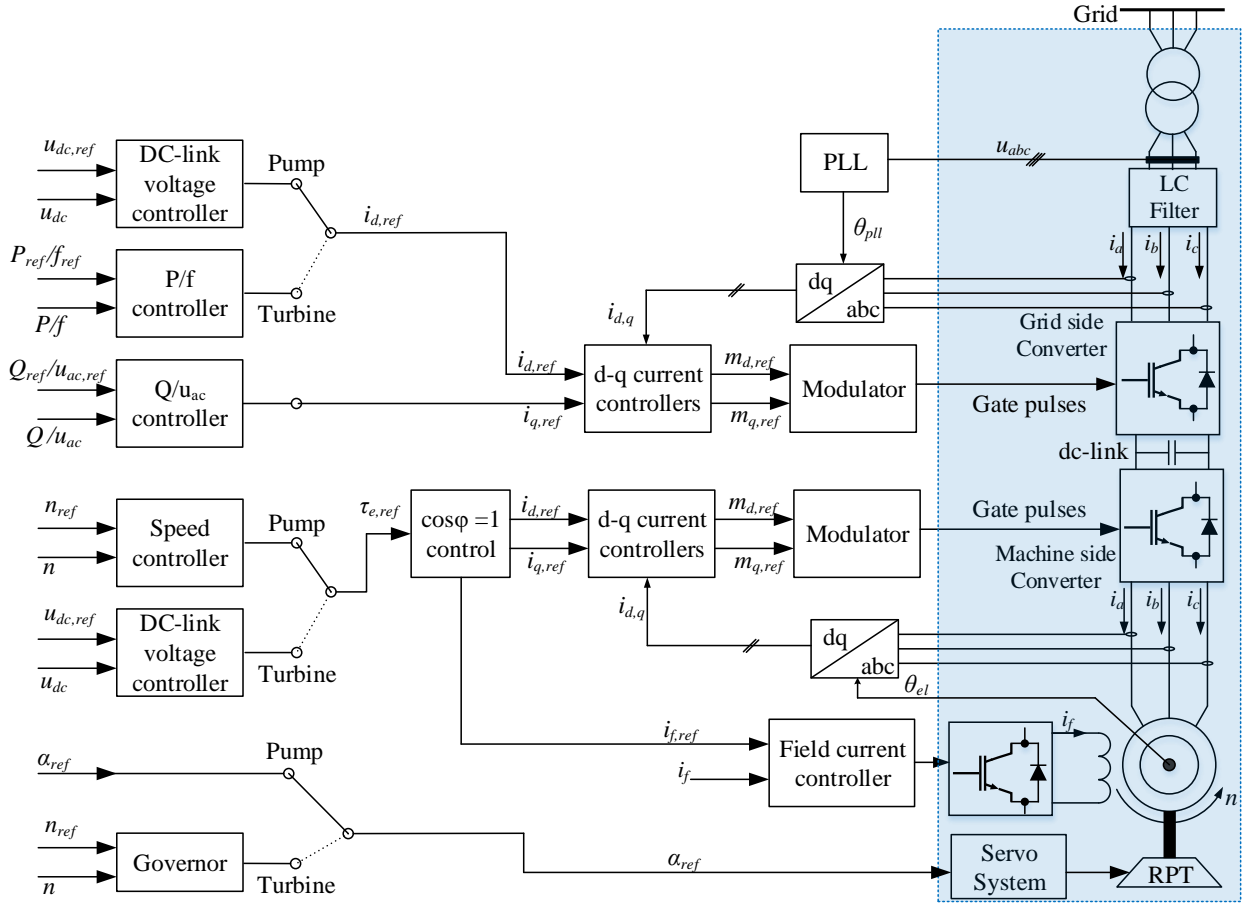


Fig. 3. Schematic of the overall control of the full-size back-to-back converters. All references to the controllers (on the left side of the figure) come from the secondary controller (presented in Fig. 2) and the Efficiency Optimization Algorithm. All controllers are proportional-integral (PI) controllers. The shaded region consists of the physical components of the power plant.

a reversible pump turbine are provided by the manufacturer or are determined experimentally using a down-scaled prototype at varying speed ( $n$ ), flow ( $Q$ ), and head ( $H$ ) as presented in [14]. The characteristic curves are popularly known as the efficiency Hill chart. The data points in the Hill chart are tabulated in a lookup table in the Efficiency Optimization Algorithm (EOA), which is part of the secondary controller or is a different entity in the outer layer of the control system. The EOA generates the speed reference both in the turbine and the pump mode to run the machine at the maximum possible efficiency. In the turbine mode, the speed is controlled by the turbine governor. The governor control system produces guide vane opening angle reference ( $\alpha_{ref}$ ) for the servo system to control the water flow to achieve the reference speed. In pump mode, the speed is controlled by the machine-side converter. The guide vanes are normally kept fully open or at an optimal opening position, and the pumping power is controlled by varying the speed.

The general control strategy for the control of the grid-side converter, machine-side converter, and governor control in both the turbine and pump mode is presented in Fig. 3.

### C. Grid-side Converter

In a conventional power plant, the synchronous machine is directly connected to the grid and the inertia of the turbine-

generator set contributes to the stability of the grid. In the case of a full-size converter-fed system, the machine setup is isolated from the grid such that the rotational speed of the turbine is independent of the grid frequency and vice versa. The grid side converter also known as the active front end (AFE) converter is now the gateway to the power flow from the machine to the grid. Utilizing the modern fast and robust control methods, virtual inertia and damping are implemented in the grid-side converter control system in order to contribute to the stability of the grid [15]–[17].

The AFE runs in different modes as demanded by the secondary layer controller. In pump mode, the AFE delivers the pumping power to the reversible pump turbine. In this mode, it controls the dc-link voltage ( $U_{dc}$ ) and supports the grid with the reactive power demanded by TSO via the secondary controller. This mode of AFE has also been referred to as the grid-following mode in literature. In turbine mode, the control variables AC voltage ( $U_{ac}$ ) and frequency ( $f$ ) are set by the secondary controller, and the variables are controlled using a synchronously rotating frame of reference as shown in Fig. 3. The control of  $U_{ac}$  in droop mode controls the reactive power ( $Q$ ) flow towards the grid whereas the frequency ( $f$ ) in droop mode controls the active power ( $P$ ). This mode of AFE is also known as a virtual synchronous machine (VSM) or grid-forming converter and provides the feature of blackout

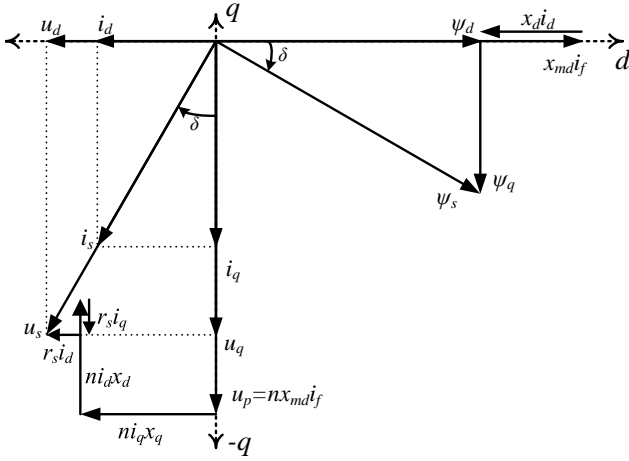


Fig. 4. Unity P. f. control of salient pole synchronous machine in pump mode of operation. The magnetic pole is aligned along the d-axis and the induced emf ( $u_p$ ) is along the negative q-axis since the speed ( $n$ ) is negative.

start of the system. In some cases, the active power ( $P_{ref}$ ) and the reactive power ( $Q_{ref}$ ) are set by the plant operator via a secondary controller, and the converter follows these references if the voltage and frequency of the grid are within the pre-specified limit.

#### D. Machine-side Converter

The machine-side converter in a PSHP controls the synchronous machine. Field-oriented control (FOC) or direct torque control (DTC) is used to control the machine. In pump mode, the speed of the machine is controlled to adjust the pumping power. The speed reference ( $n_{ref}$ ) generated by the EOA is followed to achieve maximum efficiency. In turbine mode, the speed is controlled by the turbine governor system, and the direction of the power flow changes. Since the grid-side AFE runs in grid-forming mode, the machine-side converter must control the dc-link voltage. In either mode of operation, the torque reference generated by the speed controller or the dc-link voltage controller is executed by the inner current controller.

The speed controller and the dc-link voltage controller are tuned using the Symmetrical Optimum method.

#### E. Inner Controller for Machine-side Converter

The inner controller for the machine-side converter is a torque controller. The torque reference produced by the speed or dc-link voltage controller is translated into stator current references using (1). The position of the stator current vector to achieve  $\cos \varphi = 1$  is determined by (3). Finally, the d- and q-axes current references from (4) are controlled based on sinusoidal PWM or space vector modulation technique. This control method best suits a converter-fed synchronous machine since it produces the required torque with the minimum possible stator current and converter current. Therefore, the method leads to the least possible loss in the machine and the converter at the expense of varying the field current.

The governing equation for the torque control to achieve unity power factor ( $\cos \varphi = 1$ ) is as follows based on the phasor diagram presented in Fig. 4 & 5 [18]:

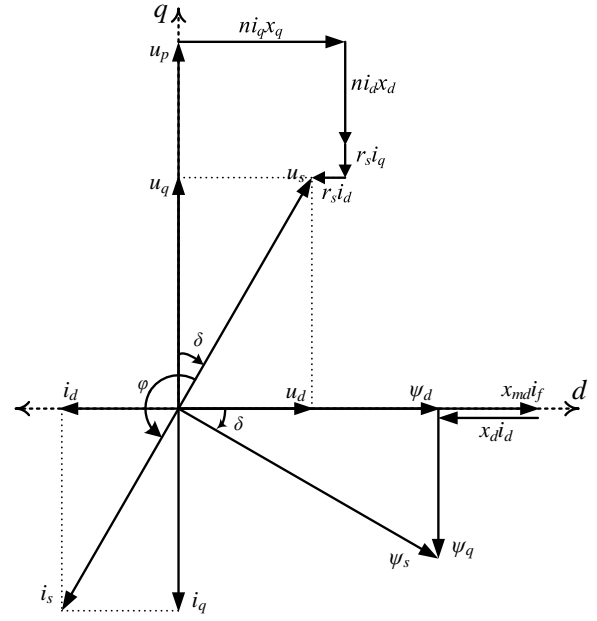


Fig. 5. Unity P. f. control of salient pole synchronous machine in turbine mode of operation. The induced emf ( $u_p$ ) is along the positive q-axis since the speed ( $n$ ) is positive.

$$\tau_e = \pm \psi_s i_s \quad (1)$$

where,  $\tau_e$  is the electrical torque,  $\psi_s$  is the stator flux linkage and  $i_s$  is the stator current of the machine in per unit. The voltage model with drift compensation is employed in this application for stator flux linkage estimation since the minimum speed limit in either direction is around 80% of the rated speed. The active power and the current out of the converter are assumed positive. Consequently, the active power ( $p$ ) out of the converter is positive in pump mode and the power into the converter is negative in turbine mode. Moreover, the speed ( $n$ ) is considered positive in turbine mode, while in pump mode, it is negative. Hence, the torque ( $\tau_e$ ) consistently remains negative in both modes of operation as:

$$p = n \cdot \tau_e \begin{cases} n > 0, \tau_e < 0 & \text{:turbine mode} \\ n < 0, \tau_e < 0 & \text{:pump mode} \end{cases} \quad (2)$$

The position of voltage and current vector ( $\delta$ ) w.r.t. the positive q-axis is calculated as:

$$\tan \delta = -\frac{x_q i_s}{\psi_s} = -\frac{\tau_e x_q}{\psi_s^2} \quad (3)$$

Based on the amplitude and position of the stator current ( $i_s$ ) from (1) and (3), respectively, the d- and q- axes current references are then calculated to pass through the current controllers to achieve the torque reference as:

$$\begin{aligned} i_d &= i_s \cdot \sin \delta \\ i_q &= -i_s \cdot \cos \delta \end{aligned} \quad (4)$$

Since the torque ( $\tau_e$ ) is always negative, the stator current ( $i_s$ ) will always be in the third quadrant, as depicted in Fig. 4 & 5, leading to both constituents  $i_d$  and  $i_q$  being negative in both turbine and pump mode of operation. The field current ( $i_f$ ) required to maintain the stator flux ( $\psi_s$ ) to the reference value for  $\cos \varphi = 1$  control can be derived from Fig. 4 or Fig.

5. Neglecting the relatively small value of the stator resistance, the field current reference is dynamically set as [18]:

$$i_f = \frac{1}{x_{md}} \frac{\psi_s^2 + x_d x_q i_s^2}{\sqrt{\psi_s^2 + x_q^2 i_s^2}} \quad (5)$$

where  $x_d$  and  $x_q$  are reactances along d- and q-axes respectively.  $x_{md}$  is the mutual inductance between field winding and d-axis winding. The field current is controlled by a separate full-bridge dc-dc converter.

All current controllers (d-axis, q-axis, and field current) are tuned using the Modulus Optimum method.

#### IV. MODELING OF REVERSIBLE PUMP TURBINE

The reversible pump turbine is the hydraulic machine that converts the water head to the mechanical torque in turbine mode. And, it generates sufficient pressure head to overcome the static water head to pump the water to the upstream reservoir in pump mode. The dynamic equations that represent the water flow ( $q$ ) based on head balance and rotational speed ( $n$ ) based on torque balance are expressed as [19], [20]:

$$T_w \frac{dq}{dt} = h - \frac{q|q|}{\kappa^2} - \sigma(|n|n - 1) - \sigma n^2 + r_q n |q| \quad (6)$$

$$T_m \frac{dn}{dt} = |q|(|q| m_s - \psi n + \sigma n - r_q |q|) - r_m n |n| - \tau_e \quad (7)$$

where  $T_w$  is the acceleration time for water depending upon the length ( $L$ ), cross-section area ( $A$ ) of the tunnel, and the rated head ( $H_0$ ) and rated flow ( $Q_0$ ) as:

$$T_w = \frac{Q_0 L}{g H_0 A} \quad (8)$$

Also,  $q$  is per unit flow through the RPT and  $n$  is the per unit angular speed.  $\kappa$  is the per unit opening of the guide vanes—0 is fully closed and 1 is fully open.  $T_m$  is the mechanical time constant of the rotating shaft, and  $r_m$  is the disk friction coefficient of the RPT.  $m_s$  is the dimensionless starting torque of the RPT as:

$$m_s = \frac{\xi}{\kappa} (\cos \alpha_1 + \tan \alpha_{1R} \sin \alpha_1) \quad (9)$$

The dimensionless parameters  $\sigma$ ,  $r_q$ ,  $\psi$ , and  $\xi$  are geometrical constants and  $\alpha_{1R}$  is the guide vanes opening at rated operation for a particular RPT, defined at its best efficiency point (BEP).  $\alpha_1$  is the opening angle of the guide vanes, and  $\tau_e$  is the per unit electrical torque of the synchronous machine.

The torque equation (7) can be rewritten as:

$$T_m \frac{dn}{dt} = \tau_{RPT} - \tau_e \quad (10)$$

Comparing (7) and (10), the torque from an RPT can be expressed as:

$$\tau_{RPT} = |q|(|q| m_s - \psi n + \sigma n - r_q |q|) - r_m n |n| \quad (11)$$

The torque from an RPT as expressed in (11) is emulated in the laboratory using a converter-controlled induction machine in combination with a real-time simulator.

#### V. EXPERIMENTAL SETUP AND RESULTS

As discussed in Section II, there exist various types of converters which can serve the purpose of the full-size converter in a back-to-back configuration. The secondary control strategy can be developed such that it is independent of the type of converter installed for the grid-side and machine-side converters. Therefore, to validate the overall system level of control, a two-level three-phase back-to-back converter setup was chosen as the laboratory prototype for this work as shown in Fig. 6.

The downscale laboratory setup consists of a synchronous machine, as in the case of fixed-speed PSHPs, and a two-level three-phase back-to-back converter set to verify the proposed control principles of this article. The field current is controlled by a separate full-bridge dc-dc converter. The field current reference ( $i_{f,ref}$ ) is set to the converter from the SM converter control board over the CAN bus. Another two-level three-phase back-to-back converter with an induction machine (IM) is connected via a gearbox (left half from the gearbox of Fig. 6) to emulate the RPT. The model of the RPT, waterway, and governor control is simulated in a real-time simulator (OPAL-RT with MATLAB Simulink models). The model also serves as the secondary controller as presented in Fig. 2 and initiates the transition of operation mode (turbine to pump or vice versa) and generates references and control mode of operation for the converters. The speed reference in the turbine mode and the torque load in pump mode are transferred to the IM converter over a high-speed optical fiber link. The IM drive control is tuned to accurately follow the simulated speed of the RPT model. The overall laboratory setup follows the control structure shown in Fig. 2 and 3, except for EOA, which was not included in the test setup. The main objective is to validate that the control principles work as proposed. The specifications of the converters and electrical machines are presented in Table I.

The following control strategies with a full-size converter setup have been experimentally verified for the control of the PSHP:

- 1) Start the machine from a standstill in turbine mode and load it to steady state load via grid side converter
- 2) Start the machine from a standstill in pump mode with water in the turbine casing and load it to the steady state value
- 3) Switch the mode of operation from pump to turbine mode without disconnecting from the grid
- 4) Switch the mode of operation from turbine to pump mode without disconnecting from the grid
- 5) Low voltage ride through in turbine mode
- 6) Low voltage ride through in pump mode

In electrical terms, the turbine and pump modes can be interchanged with generation and motoring modes, respectively. The positive speed of the synchronous machine is considered for turbine mode whereas the negative for pump mode (also shown in Fig.1).

The hydraulic parameters from an existing pumped storage plant are used to emulate the PSHP in the laboratory as presented in Table II. Since the laboratory setup has a maximum

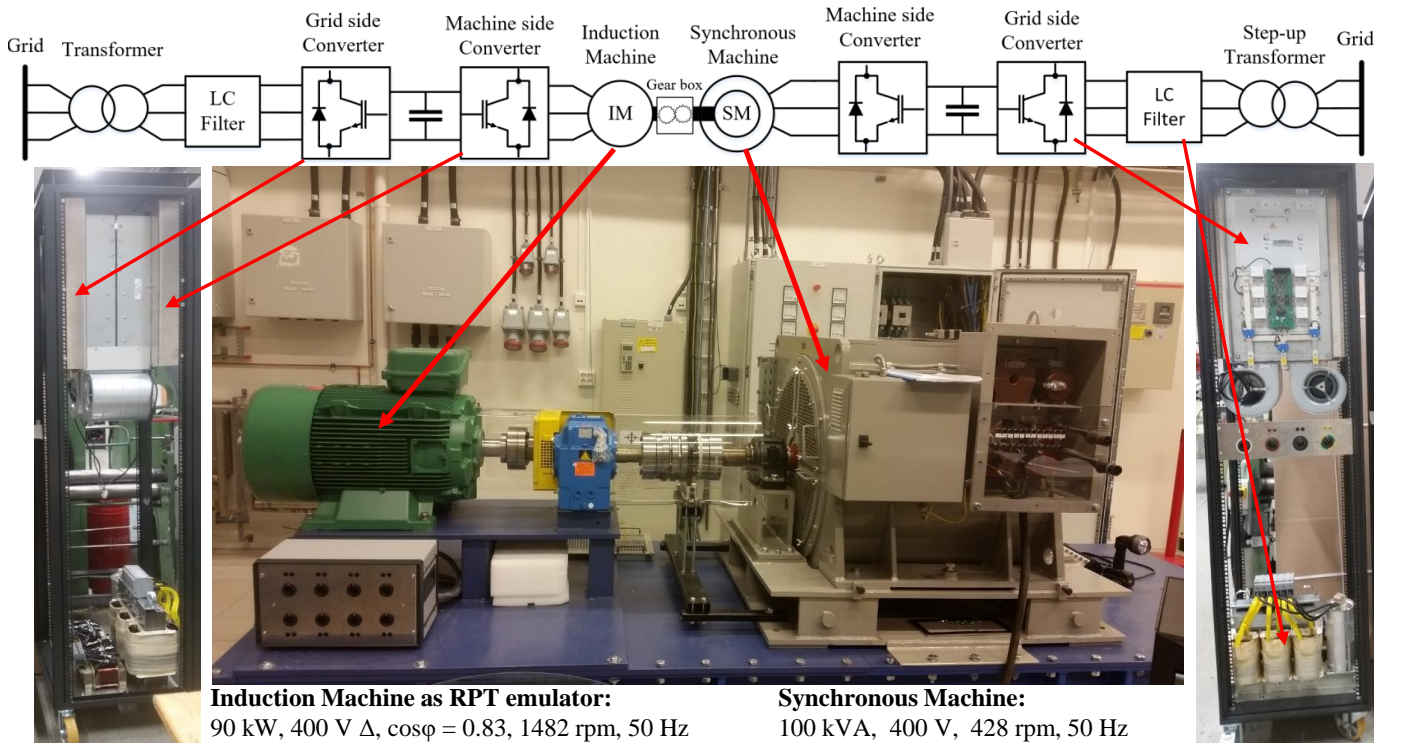


Fig. 6. 100 kVA laboratory prototype. The right half of the gearbox with a synchronous machine and back-to-back converter is the setup for which the control strategies have been proposed and tested. The left half of the gearbox with the induction machine and the back-to-back converter is emulating the reversible pump turbine.

TABLE I  
SPECIFICATION OF ELECTRICAL EQUIPMENT OF THE EXPERIMENTAL SETUP

Converter Specification - Grid side	
Rated Power	100 kVA
Rated dc-link voltage ( $U_{dc}$ )	650 V
dc-link capacitor ( $C_{dc}$ )	1.5 mF
Switching Frequency ( $f_{sw}$ )	4 kHz
Converter side inductor ( $L_1$ )	0.4 mH
AC side capacitor ( $C_{ac}$ )	27.9 $\mu$ F $\Delta$
Grid side inductor ( $L_2$ )	18 mH
Induction Machine Specification	
Rated Power	90 kW
Rated voltage	400 V
Rated current	165 A
Power factor (p.f.)	0.83
Rated speed	1482 rpm
Synchronous Machine Specification	
Rated Power	100 kVA
Rated voltage	400 V
Rated current	144.3 A
Rated speed	428.57 rpm
No. of poles	14
$x_d$	1.27 pu
$x_q$	0.75 pu
Rated field current ( $I_f$ )	56 A

All the converters are identical. The machine-side converter outputs are directly connected to the machines, whereas that of the grid-side converters are connected to the grid via an L-C-L filter.

power capacity of 90 kW, all the parameters from the PSHP model are communicated to the variable speed drives in per unit. Hence, 177 MW and 750 rpm are 1 per unit of power and speed for the RPT, which is equivalent to 90 kW and 1482

TABLE II  
HYDRAULIC PARAMETERS OF THE REFERENCE PSHP EMULATED IN THE LABORATORY

Power plant parameters (four turbines)	
Rated Power	4 $\times$ 177 MW
Rated head ( $H_0$ )	425 m
Rated discharge ( $Q_0$ )	170 $m^3/s$
Headrace Tunnel	
Length	10.65 km
Cross-section area	100 $m^2$
Water time constant	4.25 s
Penstock parameters	
Length	151.2 m
Cross-section area	6.16 $m^2$
Water time constant	1 s
Turbine parameters	
Maximum discharge ( $Q_{r,max}$ )	42.5 $m^3/s$
Rated discharge ( $Q_r$ )	38.25 $m^3/s$
Rated Head ( $H_r$ )	425 m
Rated speed ( $n$ )	750 rpm
$\sigma$	0.369
$\psi$	0.418
$\xi$	1.0
$\alpha_{1R}$	36°
Frictional coefficient ( $r_m$ )	0.05
Mechanical Time constant ( $T_m$ )	10 s

The reference power plant has four turbines and the rated head is distributed between the headrace tunnel and penstock. Only one unit is evaluated in the emulated turbine model for the experimental arrangement. The turbine parameters:  $\sigma$ ,  $\psi$ , and  $\xi$  are geometrical constants of a given turbine. The relation between these parameters is presented in the modeling equations (6) - (11).  $\alpha_{1R}$  is the opening of the guide vanes at rated discharge.

TABLE III  
LIST OF SYMBOLS USED IN FIGURES

Guide vanes opening	$\alpha$
Water flow through the RPT in per unit	$q_{pu}$
Speed of the RPT in per unit	$n_{pu}$
Electrical torque produced by the SM in per unit	$\tau_{e,pu}$
Electrical power produced by the SM in per unit	$p_{pu}$
dc-link capacitor voltage reference in per unit	$u_{dc,ref}$
Measured dc-link capacitor voltage in per unit	$u_{dc,meas}$

rpm for the induction machine of the hardware setup.

In the experimental results presented in the following sections, the electrical and mechanical parameters—d and q-axis currents ( $i_d$  and  $i_q$ ), power ( $p$ ), dc-link voltage ( $u_{dc}$ ), speed ( $n$ ), torque ( $\tau_e$ )—are measured from the hardware setup whereas the hydraulic parameters—guide vanes opening ( $\alpha$ ) and water flow ( $q$ )—are extracted from the simulation model in OPAL-RT.

The symbols used in the Figures are listed in Table III.

#### A. Startup in turbine mode from standstill

The startup process in the turbine mode is partly similar to the conventional method for a fixed-speed PSHP where the guide vanes are set to a fixed opening optimized for a particular setup (also known as idle position) and lets the machine accelerate to the nominal speed. The excitation system is then turned on. Since the rated voltage is available at the terminals, the dc-link capacitor is charged to the peak value of the ac voltage through diode rectification. The machine-side converter for the SM is then set to run state (start switching the semiconductor devices) to reach the reference dc-link voltage (which is around 0.9–1.0 pu). With a stable dc-link voltage, the AFE is started and synchronized to the grid. The experimental result of the startup process in turbine mode is presented in Fig. 7, and the response of the dc-link voltage controller is presented in Fig. 8.

In the experimental setup presented in Fig. 6, there is no external pre-charge circuit for the dc-link capacitor of the back-to-back converters. As the stator voltage builds up in turbine mode, the dc-link is charged through diode rectification of the SM side converter. Consequently, as the converter on the synchronous machine (SM) side begins switching to regulate the dc-link voltage, controller saturation induces voltage oscillation in the dc-link. This is primarily attributed to the fact that the dc-link voltage is already at the peak of the stator voltage, and there is no alternative power source to the dc-link (such as a pre-charge circuit).

#### B. Startup in pump mode from standstill

Startup in pump mode from a standstill is the major challenge of state-of-the-art pumped storage hydropower plants. In existing power plants, the water from the turbine spiral casing is compressed below the runner level so that it needs less torque to accelerate the machine to synchronous speed. There exist several methods to execute this, for example, soft starter, Load Commutated Inverter (LCI), pony motor,

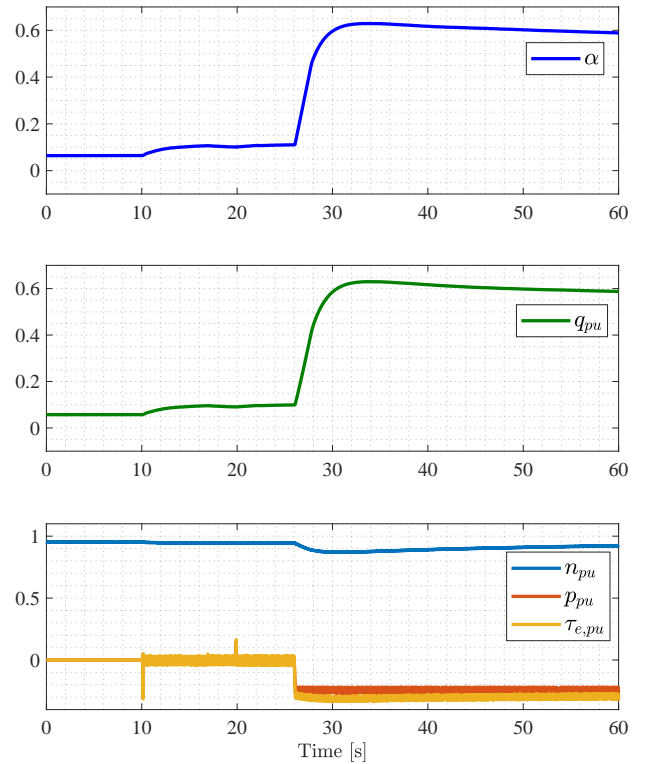


Fig. 7. Startup in turbine mode from standstill. Prior to  $t = 10$  s, the turbine governor controls the guide vanes ( $\alpha$ ) to run the turbine to 1 pu speed as in the case of a traditional fixed-speed PSHP. At  $t = 10$  s, the machine-side converter is started and the charging of the dc-link capacitor is the reason for the transient in the torque. The water flow ( $q_{pu}$ ) increases to cover the losses in the machine and the converter. At  $t = 20$  s, the grid converter is started and synchronized to the grid. At  $t = 26$  s, a power reference of -0.25 pu is set to the grid-side converter. The recovery of speed takes around 60 seconds which is completely acceptable since the grid frequency and turbine speed are decoupled.

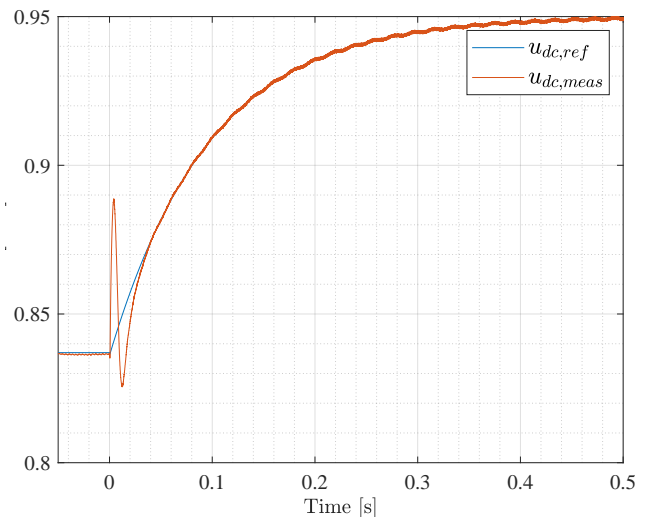


Fig. 8. Startup of synchronous machine-side (SM) converter in dc-link control. The dc-link voltage is controlled without pre-charge, which is the case during the black start of the power plant. The dc-link voltage before  $t = 0$  s is from the diode rectification of the converter. The switching is enabled at  $t = 0$  s, and the reference voltage (0.95 pu) is passed through a filter. The switching event leads to voltage oscillation caused by the saturation of the controller, which is difficult to avoid since the dc-link voltage is already at the peak of the ac voltage. The time scale of the figure differs from Fig. 7 because this event was tested separately.

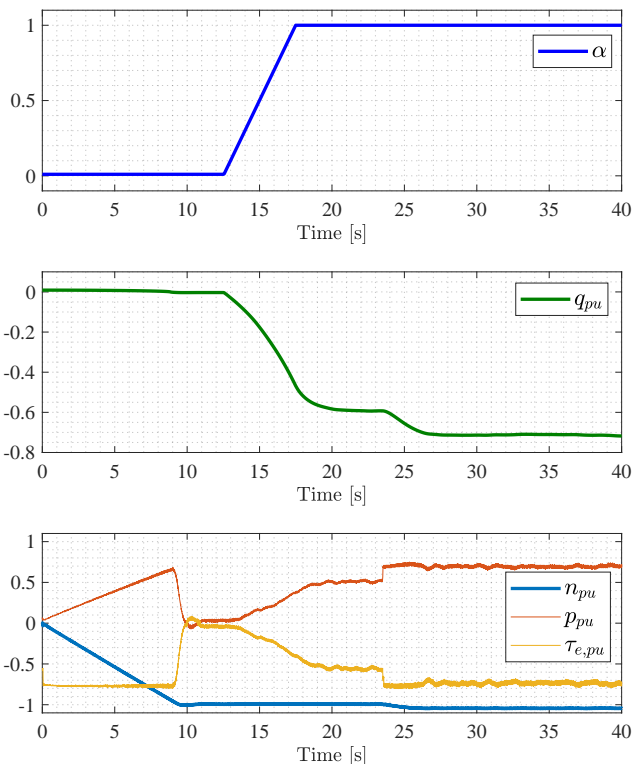


Fig. 9. Startup in pump mode from standstill. From  $t = 0s$  to  $t = 10s$ , pump speed is accelerated to -1 pu. At  $t = 12.5s$ , guide vanes have started to open and the torque loading on SM increases, and consequently, the power consumption increases. The water flow increases to -0.6 pu. At  $t = 23.5s$ , the speed reference is further increased to -1.05 pu to increase the water flow, and hence the torque loading and the power on the machine increase. The load changes sharply in this region as expected from the typical torque-speed characteristics shown in Fig. 1. The oscillation in the water flow reflects on the torque and power of the synchronous machine. It takes several minutes for the water to stabilize.

auxiliary turbine, using a rotor converter and short-circuiting the stator in a DFIM setup, and some others [21], [22].

In a PSHP with a full-size converter-fed synchronous machine, the AFE is started first in dc-link control. After the dc-link voltage stabilizes to its reference value, the machine-side converter is started in speed control mode. The RPT needs a starting torque of around 13% of its nominal torque when filled with water in the turbine casing. The machine setup is accelerated up to the rated speed at a desired rate by controlling the ramp time from the secondary controller. As the speed increases, the torque capability of the converters also increases and the speed reaches to steady state value within 5–6 mechanical time constant. The guide vanes are then opened to pump the water upstream. The speed is adjusted to control the water flow and consequently, the active power is consumed from the grid as presented in Fig. 9.

### C. Transition from the pump to turbine mode

This transition is fast even in fixed-speed PSHP as the water flows from the headrace to the tailrace once the pumping power is disconnected. The controlled transition in a converter-fed operation was tested and the result is presented in Fig. 10.

The system is running in pump mode with AFE in dc-link control mode and SM drive in the speed control with a speed in the range of -1.1 pu. When the transition of the mode

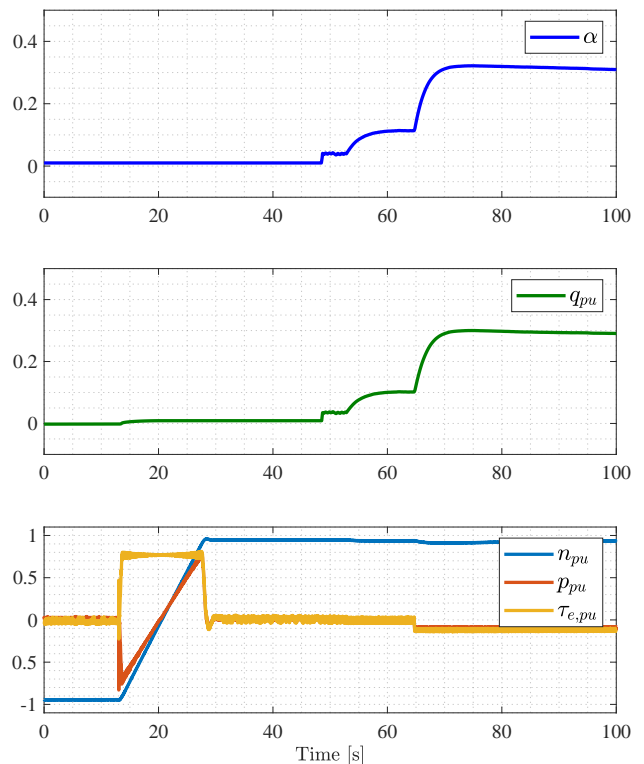


Fig. 10. Transition from pump to turbine mode. From  $t = 0s$  to  $t = 13s$ , the RPT is running in pump mode and the guide vanes have been closed to initiate the transition of the mode of operation from the pump to the turbine. At  $t = 13s$ , the secondary controller changes the speed reference from -1 to 1 pu to turn the machine in the direction of turbine mode. At  $t = 48s$ , the governor is activated for speed control. At  $t = 53s$ , the control mode of the SM converter is switched from speed control to dc-link control and the same of the grid-side converter from dc-link control to grid-connected  $u_{ac}$  and  $f_{grid}$  control. At  $t = 65s$ , the machine is loaded using grid-connected AFE.

of operation is initiated, the speed is decreased to the value where the load torque due to pumping action is minimum, i.e., the water flow is zero, and the guide vanes are closed to the minimum level (the opening level used for the start-up in generation mode) so that the pumping power consumed from the grid is close to zero. The secondary controller that initiates the mode transition changes the speed reference to 1.0 pu to turn the rotation in the direction of turbine operation. The SM drive ramps up the speed in the positive direction to the reference value. Now, the control mode of the converters is changed. The SM drive controls the dc-link voltage and the AFE remains synchronized to the grid but is now controlled as a grid-forming converter. The turbine governor is then enabled to control the speed of the machine to the reference value generated by the efficiency optimization algorithm. The power flow to the grid is now controlled by AFE running in power control mode or in frequency droop to the grid.

### D. Transition from the turbine to pump mode

The seamless transition from turbine to pump mode is not possible in a PSHP with a fixed-speed synchronous machine or with a DFIM technology because the machine must be stopped and the phase sequence of the stator connection changed to rotate the machine in the opposite direction. A full-size CFMS



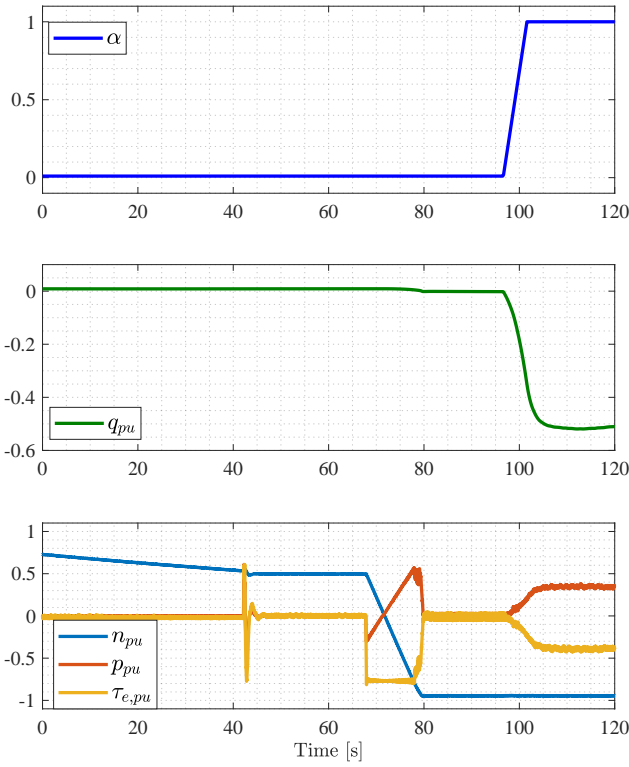


Fig. 11. Transition from turbine to pump mode. From  $t = 0s$  to  $t = 42s$ , the RPT is running in turbine mode and the guide vanes are closed to initiate the transition of mode from the turbine to pump mode. At  $t = 42s$ , the control mode of the SM converter is switched from dc-link control to speed control and the same occurs for the grid-side converter from grid-connected  $u_{ac}$  and  $f_{grid}$  control to dc-link control. At  $t = 68s$ , the secondary controller changes the speed reference from 0.5 pu to -0.93 pu to turn the machine to the pump mode direction. At  $t = 97s$ , the guide vanes are opened to pump the water.

can achieve this with the help of very fast converter control algorithms.

When the transition of operation mode from the turbine to pump mode is initiated, the AFE regulates the power to the grid close to zero and accordingly, the guide vanes come to their minimum position as the load is minimal. The control mode of converters is then switched such that AFE controls the dc-link voltage and SM drive controls the speed. Now, the speed reference is set to -1 pu and the SM drive slowly ramps down the speed to the reference value to turn the rotation to the direction of pump mode. In the experimental setup, a speed of -0.93 pu is the zero water flow point, therefore, it is set to this value. A higher speed is also allowed since the guide vanes are closed. The guide vanes are slowly opened to their maximum opening. The speed is adjusted to control the pumping power to the available power from the grid or to the power set point ( $P_{ref,pump}$ ) provided by the plant operator via the secondary controller. Since the torque loading is steep in pumping mode (as shown in Fig. 1), a small change in speed leads to a significant change in water flow and hence in pumping power.

The change of control mode of the power drives should always be carried out when the speed is positive and around 0.5 pu because crossing zero speed with SM drive in dc-link control is not possible. The rotor at zero speed does not have any power to inject into the dc-link to control the voltage to

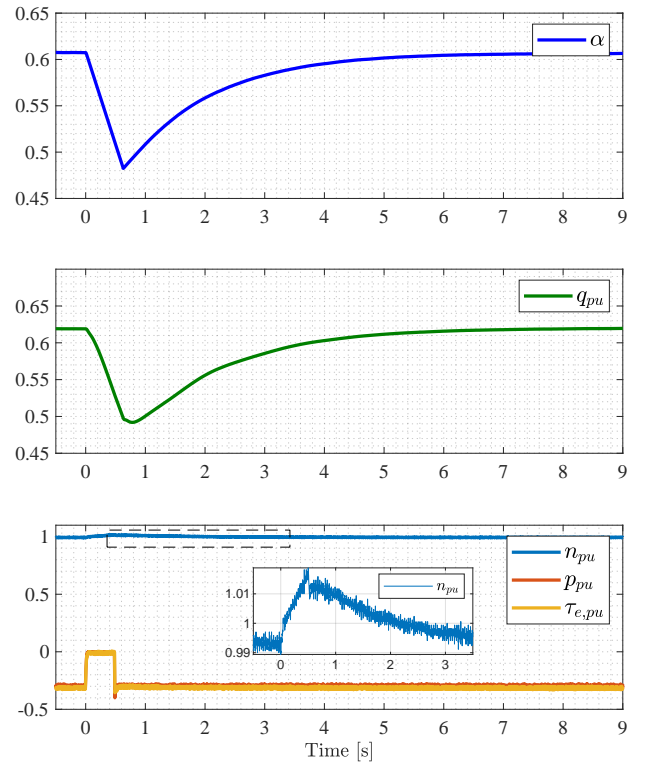


Fig. 12. Low voltage ride through in turbine mode and the response of the hydraulic system. At  $t = 0s$ , a voltage dip on the grid side occurs and the power flow from the machine to the grid is blocked. The speed increases, but the governor activates and controls the speed. After the grid is restored, the electrical torque is again impressed on the RPT, and the governor again reacts by opening the guide vanes to the pre-fault position and hence the water flow.

the reference value.

### E. Low voltage ride through in turbine mode

Low voltage ride through (LVRT) is the functionality of the grid-side converter that is capable of tolerating a voltage dip or complete short circuit for a pre-specified time according to grid-code regulations. The converter must not trip even though the voltage dips to zero for 150 ms [23], [24]. The worst-case scenario of zero voltage at AC terminals (a voltage dip of 100%) leads to the blockade of power flow from the machine to the grid. For the machine-side converter, this case is similar to the load rejection scenario in a grid-connected synchronous machine.

As presented in Fig.12, when the voltage dip occurs at  $t = 0s$ , the electrical torque production from the machine-side converter goes to zero, and hence so does the electrical power. The governor reacts immediately to control the guide vanes to maintain the reference speed of the machine, and consequently, the water flow also decreases from 0.62 pu to 0.49 pu. The fast reaction of the governor allows the machine speed to increase only by 2% as shown in the zoomed-in view of Fig.12.

In turbine mode, the machine-side converter runs in dc-link control mode and the grid-side converter in grid forming mode. When the voltage dip occurs at  $t = 0s$ , the load rejection causes a sharp rise in dc-link voltage, which in turn controls the flow of current from the machine to the converter as

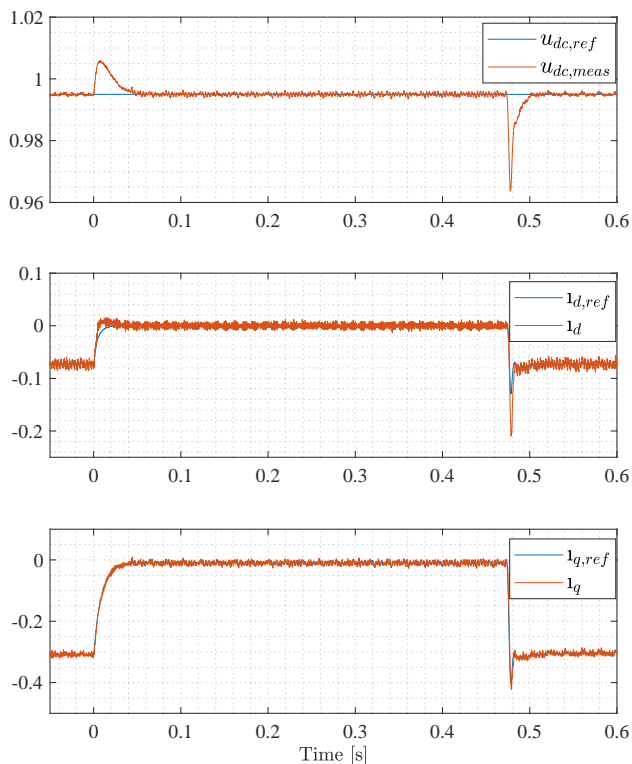


Fig. 13. Low voltage ride through in turbine mode and the response of synchronous machine drives control parameters. Here the SM drive is in dc-link voltage control. At  $t = 0s$ , a voltage dip of 100% occurs at the grid terminals and the power flow to the grid is blocked, which causes a rise in dc-link voltage. After a grid disturbance for 0.48s, the power flow is resumed and the sudden loading gives a downward spike in dc-link voltage at  $t = 0.48s$ .

shown in Fig. 13. The rise in the voltage is less than 2%. When the grid is restored at  $t = 0.48s$ , the sudden loading causes a drop of around 3% in dc-link voltage which is well within the permissible deviation. The d- and q-axes currents are controlled to zero during the voltage dip because there is no active power flow into the dc-link and the machine is magnetized only from the excitation converter.

#### F. Low voltage ride through in pump mode

When there is a voltage dip on the grid-side converter, the power available for pumping will be limited significantly due to the current rating of the semiconductor devices. The worst-case scenario is that there could be a short circuit at the AC terminals of the grid-side converter and the pumping power would be completely blocked. Since the electrical torque that is balancing the opposing torque produced by the water head disappears, the speed will decrease almost linearly with time. The mechanical time constant of the machine shaft is about 10 seconds, and therefore, the unavailability of pumping power for a duration of 0.5 seconds will lead to a 5% fall in speed. The fall in speed will lead to reduced pumping water flow as well. The guide vane remains fully open unless the short circuit prolongs and a shutdown procedure is initiated.

As shown in Fig. 14, the short circuit occurs at  $t = 0s$ . Since there is no electrical power available, the electrical torque ( $\tau_{e,pu}$ ) becomes zero, and hence so does the pumping power ( $p_{pu}$ ). The speed drops from the steady state speed of

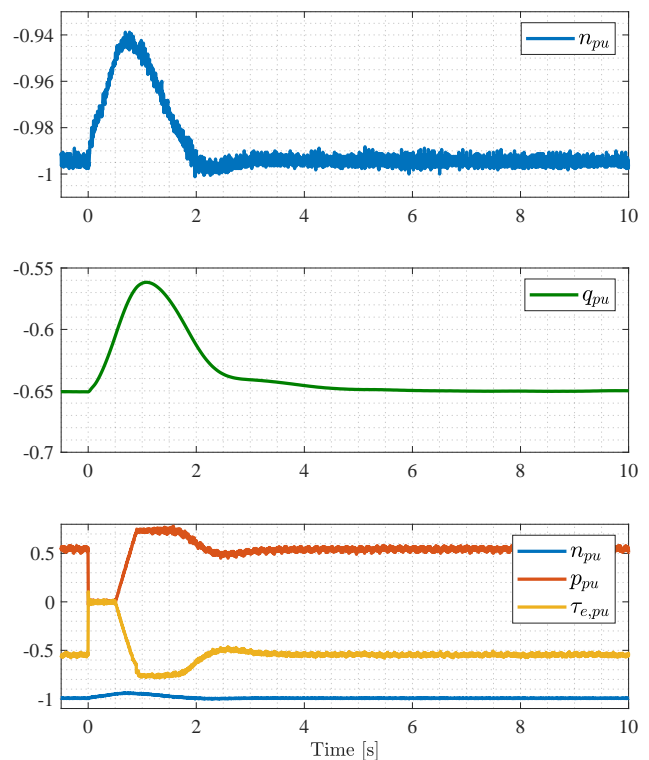


Fig. 14. Low voltage ride through in pump mode and the response of the hydraulic system. At  $t = 0s$ , a voltage dip on ac side of the grid-side converter occurs. Consequently, the electrical torque driving the machine disappears. The guide vane is fully open in pump mode, therefore, the load torque produced by the pumping head causes the speed to fall until the grid recovers at 0.5s.

$-1 pu$  to  $-0.94 pu$  and the pumping water flow decreases from  $-0.65 pu$  to  $-0.56 pu$ . After the grid is restored at  $t = 0.5s$ , the electrical torque overshoots beyond its pre-fault value to achieve the reference speed. The system stabilizes in about 10 seconds.

Some notable dynamics occur between the control parameters of the power converters as well. In pump mode, the grid-side converter controls the dc-link voltage and the machine-side converter controls the speed of the machine. During a short circuit, there is no power available to the dc-link. Consequently, the machine-side converter runs in dc-link undervoltage limitation, which draws braking power from the energy stored in the rotating shaft, to maintain the dc-link voltage at the minimum set value of  $0.91 pu$  as shown in Fig. 15. After the fault is cleared, the torque limit is slowly released for smooth loading of the grid, and the speed of the machine and dc-link voltage is restored to their pre-fault values.

The experimental results presented in Fig. 13 and 15 on the LVRT capability of the system in both turbine and pump mode show that the dc-link voltage remains within a safe limit. This is another advantage of a full-size CFM technology that an additional overvoltage protection system for the dc-link is not required compared to a DFIM solution, where a crow-bar circuit is required to handle the voltage dip at the stator terminals.

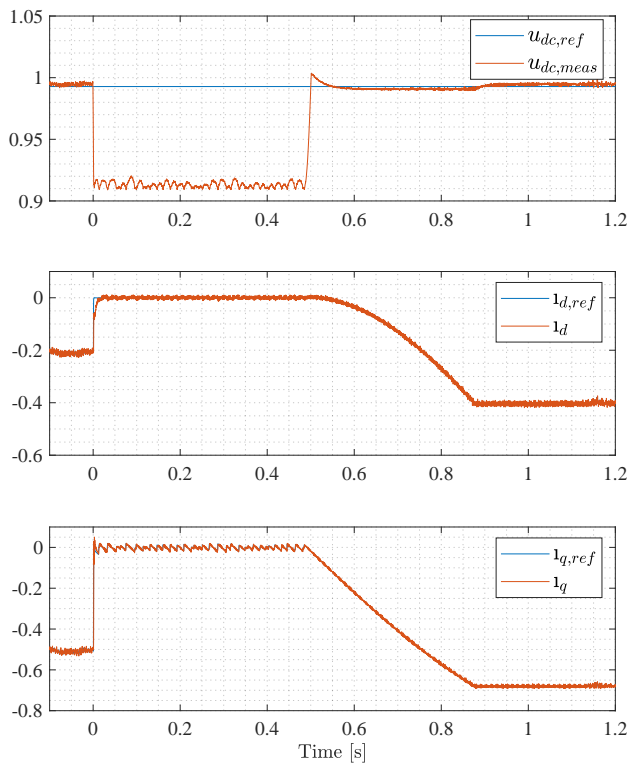


Fig. 15. Low voltage ride through in pump mode and the response of synchronous machine drives control parameters. At  $t = 0$ s, a voltage dip of 100% occurs on the grid-side converter and the power available for pumping disappears. The grid-side converter has now no power to control the dc-link voltage, therefore, the dc-link voltage also experiences a steep fall. The dc-link voltage limiter in the SM converter supplies the power needed to keep the dc-link voltage to its minimum limit value. The SM converter operates in braking mode during the voltage dip and draws energy from the rotating shaft to supply to the dc-link. The grid is restored at  $t = 0.5$ s, and the power is available on the grid side. The grid-side converter controls the dc-link voltage to the reference value and the limit on the d and q-axes currents are slowly released to continue the pumping operation.

## VI. CONCLUSION

The proposed control strategies for a full-size back-to-back converter enable a very fast control of the variable speed operation of the pumped storage plant. The startup of the plant in pump mode, which is challenging in a fixed-speed PSHP or plant with DFIM technology, is very rapid with CFMSM technology. The plant can be started within 5–6 mechanical time constant of the turbine-generator system. This control strategy can easily integrate the efficiency optimization algorithm which provides high energy savings at partial load operation compared to a fixed-speed power plant. The seamless transition of the mode of operation from the turbine to pump and vice versa within less than 100 seconds can lead to the highly efficient integration of renewable energy sources into the grid. In addition, the LVRT capability of the grid-side converter makes the system further stable and reliable in both the turbine and pump modes of operation.

The experimental results show that the system is capable of starting in turbine mode without a pre-charge circuit for the dc-link capacitor, which resembles the black start capability of a fixed-speed power plant.

## ACKNOWLEDGMENTS

The authors would like to thank the Norwegian Research Centre for Hydropower Technology - HydroCen (<https://www.ntnu.edu/hydrocen>) for supporting this work.

## REFERENCES

- [1] What are the latest trends in renewable energy? International Renewable Energy Agency (IRENA). [Online]. Available: <https://www.irena.org/Data/View-data-by-topic/Capacity-and-Generation/Statistics-Time-Series>
- [2] J. Pérez-Díaz, G. Cavazzini, F. Blázquez, C. Platero, J. Fraile-Ardanuy, J. Sánchez, and M. Chazarra, "Technological developments for pumped-hydro energy storage, Mechanical Storage Subprogramme, Joint Programme on Energy Storage," European Energy Research Alliance, Technical Report, May 2014.
- [3] P. K. Steimer, O. Senturk, S. Aubert, and S. Linder, "Converter-fed synchronous machine for pumped hydro storage plants," in *2014 IEEE Energy Conversion Congress and Exposition (ECCE)*, 2014, pp. 4561–4567.
- [4] M. Valavi and A. Nysveen, "Variable-Speed Operation of Hydropower Plants: A Look at the Past, Present, and Future," *IEEE Industry Applications Magazine*, vol. 24, no. 5, pp. 18–27, 2018.
- [5] H. Schlunegger and A. Thöni, "100MW full-size converter in the Grimsel 2 pumped-storage plant," *Innsbruck, Hydro*, 2013.
- [6] A. Christe, A. Faulstich, M. Vasiladiotis, and P. Steinmann, "World's First Fully-Rated Direct ac/ac MMC for Variable-Speed Pumped-Storage Hydropower Plants," *IEEE Transactions on Industrial Electronics*, pp. 1–10, 2022.
- [7] Y. Pannatier, B. Kawkabani, C. Nicolet, J. Simond, A. Schwery, and P. Allenbach, "Investigation of Control Strategies for Variable-Speed Pump-Turbine Units by Using a Simplified Model of the Converters," *IEEE Transactions on Industrial Electronics*, vol. 57, pp. 3039–3049, 2010.
- [8] M. Basić, A. Schwery, and D. Dujčić, "Highly Flexible Indirect Modular Multilevel Converter for High Power Pumped Hydro Storage Plants," in *IECON 2020 The 46th Annual Conference of the IEEE Industrial Electronics Society*, 2020, pp. 5290–5295.
- [9] R. Tiwari, R. Nilsen, and O. Mo, "Control Strategies for Variable Speed Operation of Pumped Storage Plants with Full-size Converter Fed Synchronous Machines," in *2021 IEEE Energy Conversion Congress and Exposition (ECCE)*, 2021, pp. 61–68.
- [10] "Asymmetric and reverse conducting (IGCTs) | Hitachi ABB," [online].
- [11] R. Tiwari, R. Nilsen, and A. Nysveen, "Evaluation and comparison between multilevel converters for variable speed operation of pumped storage power plants with full-size converters," in *2021 IEEE Industry Applications Society Annual Meeting (IAS)*, 2021, pp. 1–8.
- [12] R. Tiwari, R. Nilsen, and A. Nysveen, "Active NPC Converter for Variable Speed Operation of Pumped Storage Hydropower Plant," in *IECON 2020 The 46th Annual Conference of the IEEE Industrial Electronics Society*, Singapore, 2020, pp. 1211–1216.
- [13] M. Hagiwara, I. Hasegawa, and H. Akagi, "Start-up and low-speed operation of an electric motor driven by a modular multilevel cascade inverter," *IEEE Transactions on Industry Applications*, vol. 49, no. 4, pp. 1556–1565, 2013.
- [14] P. Guo, Z. Wang, L. Sun, and X. Luo, "Characteristic analysis of the efficiency hill chart of Francis turbine for different water heads," *Advances in Mechanical Engineering*, vol. 9, no. 2, p. 8, 2017. [Online]. Available: <https://doi.org/10.1177/1687814017690071>
- [15] S. D'Arco and J. A. Suul, "Virtual synchronous machines — classification of implementations and analysis of equivalence to droop controllers for microgrids," in *2013 IEEE Grenoble Conference*, 2013, pp. 1–7.
- [16] —, "Equivalence of virtual synchronous machines and frequency-droops for converter-based microgrids," *IEEE Transactions on Smart Grid*, vol. 5, no. 1, pp. 394–395, 2014.
- [17] S. D'Arco, J. A. Suul, and O. B. Fosfo, "A Virtual Synchronous Machine implementation for distributed control of power converters in SmartGrids," *Electric Power Systems Research*, vol. 122, pp. 180–197, 2015.
- [18] H. Bühler, *Einführung in die Theorie Geregelter Drehstromantriebe: Band 2. Anwendungen*, ser. Lehrbücher der Elektrotechnik. Birkhäuser Basel, 1977. [Online]. Available: <https://www.springer.com/gp/book/9783034864428>

- [19] T. K. Nielsen, "Simulation model for Francis and Reversible Pump Turbines," *International Journal of Fluid Machinery and Systems*, vol. 8, no. 3, pp. 169–182, 2015.
- [20] M. F. Svarstad, "Fast Transition between Operational Modes of a reversible Pump-Turbine," PhD Thesis, Norwegian University of Science and Technology (NTNU), 2019.
- [21] T. J. Hammons and J. Loughran, "Starting methods for generator/motor units employed in pumped-storage stations," *Proceedings of the Institution of Electrical Engineers*, vol. 117, no. 9, pp. 1829–1840, Sep. 1970.
- [22] K. Gamlesaeter, "Starting methods for pump storage units," in *Cigre*, Paris, France, 1991.
- [23] G. Joos, "Wind turbine generator low voltage ride through requirements and solutions," in *2008 IEEE Power and Energy Society General Meeting - Conversion and Delivery of Electrical Energy in the 21st Century*, 2008, pp. 1–7.
- [24] Y. Bak, J.-S. Lee, and K.-B. Lee, "Low-Voltage Ride-Through Control Strategy for a Grid-Connected Energy Storage System," *Applied Sciences*, vol. 8, no. 1, 2018. [Online]. Available: <https://www.mdpi.com/2076-3417/8/1/57>



**Raghendra Tiwari** received his Bachelor's degree in Electrical Engineering from the Pulchowk Campus, Tribhuvan University, Nepal, in 2005, and his M.Sc. degree in Electric Power Engineering from the Norwegian University of Science and Technology (NTNU), Trondheim, Norway, in 2012. He is currently working toward his Ph.D. degree at the Department of Electric Energy, NTNU. From 2006 to 2010, he worked in hydropower; and from 2011 to 2017, he was with Wärtsilä Norway AS, working with the development of MW-scale low-voltage converters for marine applications. His current research interests include variable speed drive control, hybrid systems, and energy storage technologies.



**Roy Nilsen** received the M.Sc. degree in 1984, and the Ph.D. degree in 1987 from the Norwegian Institute of Technology (NTH). In the period 1987–1996, he was employed with ABB. From 1988 to 1989, he was with ABB Drives in Turgi, Switzerland. From 1989 until 1996, he was with ABB Corporate Research in Oslo, Norway. In the period 1996–2006, he was a Professor in Electric Drives with the Norwegian University of Science and Technology (NTNU), Trondheim, Norway. From 2001 until 2017, he has been participating in developing drives for marine applications in Aker/Wärtsilä/The Switch. Since April 2017, he is back as a Professor in Electric Drives with the Department of Electric Energy, NTNU. He is the head of the Power Electronic Systems and Components (PESC) research group at the department.



**Olve Mo** was born in Norway in 1965. He received the M.Sc. and Dr.Eng. degrees in electrical engineering from the Norwegian Institute of Technology, Trondheim, Norway, in 1988 and 1993, respectively. Since 2014, he has been with SINTEF Energy Research, Trondheim, Norway, where he is currently a Research Scientist. His former experience includes eight years at Marine Cybernetics, developing simulator-based testing technology for control systems software on advanced offshore vessels, five years former employment at SINTEF Energy Research, five years at Siemens, Trondheim, Norway, working with switchgear deliveries to the oil and gas industry, and two years as an Associate Professor at the High Voltage Section, Norwegian University of Science and Technology. His current research interests are related to power converters and energy storage in power systems, including wind farms and marine propulsion systems.



**Arne Nysveen** received the M.Sc. and Dr.Eng. (Ph.D.) degrees in electric power engineering from the Norwegian Institute of Technology (now Norwegian University of Science and Technology), Trondheim, Norway, in 1988 and 1994, respectively. From 1995 to 2002, he was a Senior Scientist with ABB Corporate Research, Oslo, Norway. Since 2002, he has been a Professor at the Norwegian University of Science and Technology, where he is currently a Manager for research on turbine and generator technologies with the Norwegian Research Center for Hydropower Technology (HydroCen). His current research interests include the design, modeling, and monitoring of hydroelectric generators.